JOURNAL OF THERMOPHYSICS AND HEAT TRANSFER
Vol. 21, No. 1, January–March 2007

Modified Temperature-Transforming Model for Convection-Controlled Melting

Piyasak Damronglerd* and Yuwen Zhang†
University of Missouri-Columbia, Columbia, Missouri 65211

DOI: 10.2514/1.21529

The temperature-transforming model developed in the 1990s is capable of solving convection-controlled solid-liquid phase-change problems. In this methodology, phase change is assumed to take place gradually through a range of temperatures. The heat capacity within the range of phase-change temperatures was assumed to be average to that of solid and liquid in the original temperature-transforming model. In this paper, a modified temperature-transforming model is proposed, to consider the dependence of heat capacity on the fractions of solid and liquid in the mushy zone. The ramped switch-off method is used for a solid velocity-correction scheme. The results are then compared with existing experimental and numerical results for a melting problem is a rectangular cavity. The results show that the modified model is closer to experimental results with octadecane as pulse code modulation, even though its heat capacity ratio is close to one. The modified model is then tested on substances that have heat capacity further from one, such as 0.4437 for water and 1.2034 for acetic acid. The results show that the original model underpredicts the velocity of the solid–liquid interface when the heat capacity ratio is less than one and overpredicts the velocity when the ratio is higher than one.

Nomenclature

C	=	c^0/c_l
C_{sl}	=	solid–liquid heat capacity ratio, c_s/c_l
c	=	specific heat, J/(kg · K)
c^0	=	coefficient, J/(kg · K)
d	=	coefficient in velocity correction
g	=	gravitational acceleration, 9.8 m/s^2
H	=	height of the vertical wall, m
K	=	dimensionless thermal conductivity, k/k_l
K_{sl}	=	ratio of thermal conductivities, k_s/k_l
k	=	thermal conductivity, W/(m · K)
L	=	latent heat, J/kg
L_x, L_y	=	number of nodes on the X and Y direction
P	=	dimensionless pressure, $(p + \rho_\infty gy)H^2/\rho\nu_l^2$
P^*	=	initially guessed dimensionless pressure
P'	=	dimensionless pressure correction
Pr	=	Prandtl number, ν/α_l
Pr_l	=	Prandtl number of liquid, ν_l/α_l
p	=	pressure, N/m^2
Q_c	=	dimensionless average heat transfer rate on the right wall, $q_c''H/k_s(T_h^0 - T_m^0)$
Q_h	=	dimensionless average heat transfer rate on the left wall, $q_h''H/k_l(T_h^0 - T_m^0)$
q_c''	=	average heat transfer rate on the right wall, W/m^2
q_h''	=	average heat transfer rate on the left wall, W/m^2
Ra	=	$g\beta H^3(T_h^0 - T_m^0)/\nu_l\alpha_l$
S	=	$S^0/c_l(T_h^0 - T_m^0)$
Sc	=	subcooling parameter, $(T_c^0 - T_m^0)/(T_h^0 - T_m^0)$
S_C	=	linearized source term
S_P	=	linearized source term
Ste	=	Stefan number, $c_l(T_h^0 - T_m^0)/h_{\mathrm{sl}}$
S^0	=	source term
T	=	dimensionless temperature, $(T^0 - T_m^0)/(T_h^0 - T_m^0)$
T_i	=	dimensionless initial temperature
T^0	=	temperature, K
T_c^0	=	cold surface temperature, K
T_h^0	=	hot surface temperature, K
T_m^0	=	melting (or freezing) temperature, K
t	=	time, s
U, V	=	dimensionless velocities, uH/ν_l, vH/ν_l
u, v	=	velocities, m/s
V_L	=	melting rate
X, Y	=	dimensionless coordinate directions, x/H, y/H
x, y	=	coordinate, m
α	=	thermal diffusivity, m^2/s
β	=	coefficient of volumetric thermal expansion, 1/K
ΔT	=	$\Delta T^0/(T_h^0 - T_m^0)$
ε_l	=	ratio of the volume of liquid to the total volume of the computational domain
μ	=	dynamic viscosity, kg/(m · s)
ν	=	kinematic viscosity, m^2/s
ρ	=	density, kg/m^3, $\rho = \rho_\infty[1 - \beta(T^0 - T_m^0)]$
ρ_∞	=	reference density, kg/m^3
τ	=	dimensionless time, $\nu_l t/\mathrm{H}^2$
ϕ	=	general dependent variable
$2\Delta T^0$	=	phase-change temperature range, K

Subscripts

E	=	east neighbor of grid P
e	=	control-volume face between P and E
i	=	initial value
l	=	liquid phase
m	=	mushy phase
N	=	north neighbor of grid P
n	=	control-volume face between P and N
nb	=	neighbors of grid P
P	=	grid point
S	=	south neighbor of grid P
s	=	solid phase or control-volume face between P and S
W	=	west neighbor of grid P
w	=	control-volume face between P and W

Received 2 December 2005; revision received 20 July 2006; accepted for publication 13 August 2006.

*Graduate Research Assistant, Department of Mechanical and Aerospace Engineering.

†Associate Professor, Department of Mechanical and Aerospace Engineering. Senior Member AIAA.

I. Introduction

PHASE-CHANGE heat transfer has received considerable attention in literature [1,2] due to its importance in latent heat

thermal energy storage devices [3–5] and many other applications. Many numerical models for melting and solidification of various phase-change materials (PCMs) have been developed. The numerical models can be divided into two groups [6]: *deforming grid schemes* (or strong numerical solutions) and *fixed grid schemes* (or weak numerical solutions). Deforming grid schemes transform solid and liquid phases into fixed regions by using a coordinate transformation technique. The governing equations and boundary conditions are complicated due to the transformation. These schemes have successfully solved multidimensional problems with or without natural convection. The disadvantage of deforming grid schemes is that they require significant amount of computational time. On the other hand, fixed grid schemes use one set of governing equations for the whole computational domain, including both liquid and solid phases, and the solid–liquid interface is later determined from the temperature distribution. This simplicity makes the computation much faster than deforming grid schemes, and it still provides reasonably accurate results [7]. There are two main methods in the fixed grid schemes: the enthalpy method and the equivalent heat capacity method. The enthalpy method [8] can solve heat transfer in the mushy zone but has difficulty with temperature oscillation, whereas the equivalent heat capacity method [9,10] requires large enough temperature range in the mushy zone to obtain converged solution.

Cao and Faghri [11] combined the advantages of both enthalpy and equivalent heat capacity methods and proposed a temperature-transforming model (TTM) that could also account for natural convection. TTM converts the enthalpy-based energy equation into a nonlinear equation with a single dependent variable: temperature. To use the TTM in solid–liquid phase-change problems, it is necessary to make sure that the velocity in the solid region is zero. In the liquid region, the velocity must be solved from the corresponding momentum and continuity equations. There are three widely used velocity-correction methods [12]: switch-off method (SOM) [13], source term method (STM), and variable viscosity method (VVM). Voller [12] compared these three methods and concluded that STM is the most stable method for phase-change problems. Ma and Zhang [14] proposed two modified methods that can be used with TTM: the ramped switch-off method (RSOM) and the ramped source term method (RSTM). These two methods were modified from the original SOM and STM in order to eliminate discontinuity between the two phases. Because RSOM and RSTM give virtually the same results, this paper follows the recommendations of [14] and uses the RSOM method for velocity treatment in solid.

The heat capacity within the range of phase-change temperature was assumed to be average to that of solid and liquid in the original TTM. Although this treatment could provide accurate results for the cases where the heat capacity ratio of the PCM is close to one ($\rho_s c_{ps} \approx \rho_\ell c_{p\ell}$), an alternative method that can consider the dependence of heat capacity on the fractions of solid and liquid in the mushy zone is necessary for the case where the heat capacity ratio is not close to one. A modified TTM that considers heat capacity in the mushy zone as a linear function of solid and liquid fractions will be developed in this paper.

II. Governing Equations

The TTM that was proposed by Cao and Faghri [11] is based on the following assumptions:

1) Solid–liquid phase change occurred within a range of temperatures.

2) The fluid flow in the liquid phase is an incompressible laminar flow with no viscous dissipation.

3) The change of thermal physical properties in the mushy region is linear., and

4) The thermal physical properties are constants in each phase, but may differ among solid and liquid phases, whereas density is constant for all phases.

Melting inside a rectangular enclosure, as shown in Fig. 1, will be studied in this paper. The top and bottom walls are insulated, whereas the left and right walls are kept at constant T_h^0 and constant T_c^0. The

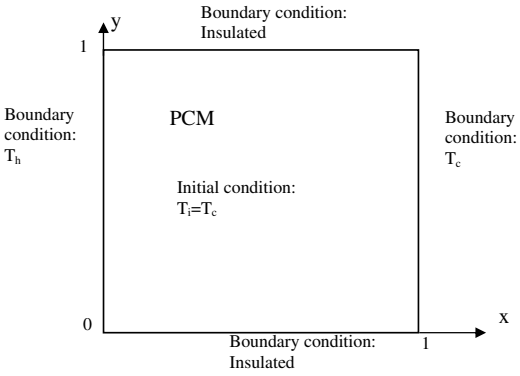

Fig. 1 Melting in a two-dimensional cavity.

initial temperatures were set to T_c^0 in all cases. In TTM, conventional continuity and momentum equations for fluid flow problems are applicable, whereas the energy equation is transformed into a nonlinear equation similar to the method used in temperature-based equivalent heat capacity methods. Under the assumption that there is no density change during phase change and the liquid phase is incompressible, the governing equations using the original TTM expressed in a two-dimensional Cartesian coordinate system are as follows (y axis is the vertical axis):

continuity equation

$$\frac{\partial u}{\partial x} + \frac{\partial v}{\partial y} = 0 \tag{1}$$

momentum equations in x and y directions

$$\frac{\partial(\rho u)}{\partial t} + \frac{\partial(\rho u u)}{\partial x} + \frac{\partial(\rho v u)}{\partial y} = -\frac{\partial p}{\partial x} + \frac{\partial}{\partial x}\left(\mu \frac{\partial u}{\partial x}\right) + \frac{\partial}{\partial y}\left(\mu \frac{\partial u}{\partial y}\right) \tag{2}$$

$$\frac{\partial(\rho v)}{\partial t} + \frac{\partial(\rho u v)}{\partial x} + \frac{\partial(\rho v v)}{\partial y} = -\frac{\partial p}{\partial y} + \rho g + \frac{\partial}{\partial x}\left(\mu \frac{\partial v}{\partial x}\right) + \frac{\partial}{\partial y}\left(\mu \frac{\partial v}{\partial y}\right) \tag{3}$$

energy equation

$$\frac{\partial(C^0 T^0)}{\partial t} + \frac{\partial(C^0 u T^0)}{\partial x} + \frac{\partial(C^0 v T^0)}{\partial y} = \frac{\partial}{\partial x}\left(k \frac{\partial T^0}{\partial x}\right) + \frac{\partial}{\partial y}\left(k \frac{\partial T^0}{\partial y}\right) - \left[\frac{\partial S^0}{\partial t} + \frac{\partial(u S^0)}{\partial x} + \frac{\partial(v S^0)}{\partial y}\right] \tag{4}$$

where coefficients C^0 and S^0 in Eq. (4) are

$$C^0(T) = \begin{cases} (\rho c)_s, & T^0 < T_m^0 - \Delta T^0 \\ (\rho c)_m + \frac{\rho h_{sl}}{2\Delta T^0}, & T_m^0 - \Delta T^0 \le T^0 \le T_m^0 + \Delta T^0 \\ (\rho c)_l, & T^0 > T_m^0 + \Delta T^0 \end{cases} \tag{5}$$

$$S^0(T) = \begin{cases} (\rho c)_s \Delta T^0, & T^0 < T_m^0 - \Delta T^0 \\ (\rho c)_m \Delta T^0, & T_m^0 - \Delta T^0 \le T^0 \le T_m^0 + \Delta T^0 \\ (\rho c)_l \Delta T^0 + \rho h_{sl}, & T^0 > T_m^0 + \Delta T^0 \end{cases} \tag{6}$$

and the thermal conductivity is

$$K(T) = \begin{cases} k_s, & T^0 < T_m^0 - \Delta T^0 \\ k_s + (k_l - k_s)\frac{T^0 - T_m^0 + \Delta T^0}{2\Delta T^0}, & T_m^0 - \Delta T^0 \le T^0 \le T_m^0 + \Delta T^0 \\ k_l, & T^0 \le T_m^0 + \Delta T^0 \end{cases} \tag{7}$$

where $T^0 < T_m^0 - \Delta T^0$ corresponds to the solid phase,

$$T_m^0 - \Delta T^0 \le T^0 \le T_m^0 + \Delta T^0$$

to the mushy zone, and $T^0 > T_m^0 + \Delta T^0$ to the liquid phase. The heat capacity in the mushy zone was assumed to be the average of those of solid and liquid phases:

$$(\rho c)_m = \tfrac{1}{2}[(\rho c)_s + (\rho c)_l] \tag{8}$$

which will not be a suitable assumption when the heat capacity ratio of the substance is not close to one. To improve the TTM, it is proposed that the heat capacity is a function of the liquid fraction:

$$(\rho c)_m = (1 - \varphi_l)(\rho c)_s + \varphi_l (\rho c)_l \tag{9}$$

where φ_l is liquid fractions in the mushy zone and the solid fraction is $1 - \varphi_l$. Because the mushy zone has temperatures from $T_m^0 - \Delta T^0$ to $T_m^0 + \Delta T^0$, the liquid fraction is a linear function of the temperature of the mushy zone by

$$\varphi_l = \frac{T^0 - T_m^0 + \Delta T^0}{2\Delta T^0} \tag{10}$$

The coefficients C^0 and S^0 for the energy equation of the modified TTM become

$$C^0(T^0) = \begin{cases} (\rho c)_s, & T^0 - T_m^0 < -\Delta T^0 \\ \frac{(\rho c)_l + (\rho c)_s}{2} + \frac{\rho h_{sl}}{2\Delta T^0} + \frac{(\rho c)_l - (\rho c)_s}{4}(T^0 - T_m^0), & -\Delta T^0 \le T^0 - T_m^0 \le \Delta T^0 \\ (\rho c)_l, & T^0 - T_m^0 > \Delta T^0 \end{cases} \tag{11}$$

$$S^0(T^0) = \begin{cases} (\rho c)_s \Delta T^0, & T^0 - T_m^0 < -\Delta T^0 \\ \frac{(\rho c)_l + 3(\rho c)_s}{4}\Delta T^0 + \frac{\rho h_{sl}}{2}, & -\Delta T^0 \le T^0 - T_m^0 \le \Delta T^0 \\ (\rho c)_s \Delta T^0 + \rho h_{sl}, & T^0 - T_m^0 > \Delta T^0 \end{cases} \tag{12}$$

and the thermal conductivity is

$$k(T^0) = \begin{cases} k_s, & T^0 - T_m^0 < -\Delta T^0 \\ \frac{k_l + k_s}{2} + \frac{(k_l - k_s)}{2\Delta T^0}(T^0 - T_m^0), & -\Delta T^0 \le T^0 - T_m^0 \le \Delta T^0 \\ k_l, & T^0 - T_m^0 > \Delta T^0 \end{cases} \tag{13}$$

Introducing the following nondimensional variables

$$\begin{aligned} X &= \frac{x}{H}, \quad Y = \frac{y}{H}, \quad U = u\frac{H}{\nu_l}, \quad V = v\frac{H}{\nu_l} \\ T &= \frac{T^0 - T_m^0}{T_h^0 - T_m^0}, \quad \Delta T = \frac{\Delta T^0}{T_h^0 - T_m^0}, \quad C = \frac{C^0}{(\rho c)_l} \\ S &= \frac{S^0}{(\rho c)_l (T_h^0 - T_m^0)}, \quad K = \frac{k}{k_l}, \quad Ste = \frac{c_l (T_h^0 - T_m^0)}{h_{sl}} \\ C_{sl} &= \frac{(\rho c)_s}{(\rho c)_l}, \quad K_{sl} = \frac{k_s}{k_l}, \quad P = \frac{H^2}{\rho \nu_l^2}(p + \rho g) \end{aligned} \tag{14}$$

The governing equations can be nondimensionalized as

$$\frac{\partial U}{\partial X} + \frac{\partial V}{\partial Y} = 0 \tag{15}$$

$$\frac{\partial U}{\partial \tau} + \frac{\partial (U^2)}{\partial X} + \frac{\partial (UV)}{\partial Y} = -\frac{\partial P}{\partial X} + \frac{\partial}{\partial \mathrm{X}}\left(\frac{Pr}{Pr_l}\frac{\partial U}{\partial X}\right) + \frac{\partial}{\partial \mathrm{Y}}\left(\frac{Pr}{Pr_l}\frac{\partial U}{\partial Y}\right) \tag{16}$$

$$\frac{\partial V}{\partial \tau} + \frac{\partial (UV)}{\partial X} + \frac{\partial (V^2)}{\partial Y} = -\frac{\partial P}{\partial Y} + \frac{Ra}{Pr_l}T + \frac{\partial}{\partial X}\left(\frac{Pr}{Pr_l}\frac{\partial V}{\partial X}\right) + \frac{\partial}{\partial Y}\left(\frac{Pr}{Pr_l}\frac{\partial V}{\partial Y}\right) \tag{17}$$

$$\frac{\partial (CT)}{\partial \tau} + \frac{\partial (UCT)}{\partial X} + \frac{\partial (VCT)}{\partial Y} = \frac{\partial}{\partial X}\left(\frac{K}{Pr_l}\frac{\partial T}{\partial X}\right) + \frac{\partial}{\partial Y}\left(\frac{K}{Pr_l}\frac{\partial T}{\partial Y}\right) - \left[\frac{\partial S}{\partial \tau} + \frac{\partial (US)}{\partial X} + \frac{\partial (VS)}{\partial Y}\right] \tag{18}$$

where

$$C = \begin{cases} C_{sl}, & T < -\Delta T \\ \frac{1 + C_{sl}}{2} + \frac{1}{2Ste\Delta T} + \frac{1 - C_{sl}}{4\Delta T}T, & -\Delta T \le T \le \Delta T \\ 1, & T > \Delta T \end{cases} \tag{19}$$

$$S = \begin{cases} C_{sl}\Delta T, & T < -\Delta T \\ \frac{1 + 3C_{sl}}{4}\Delta T + \frac{1}{2Ste}, & -\Delta T \le T \le \Delta T \\ C_{sl}\Delta T + \frac{1}{Ste}, & T > \Delta T \end{cases} \tag{20}$$

and the thermal conductivity is

$$K = \begin{cases} K_{sl}, & T < -\Delta T \\ \frac{1 + K_{sl}}{2} + \frac{1 - K_{sl}}{2\Delta T}T, & -\Delta T \le T \le \Delta T \\ 1, & T > \Delta T \end{cases} \tag{21}$$

It should be noted that the body force in Eq. (17) will be changed to $Ra|T - T_{\max}|^q/Pr$ when the working fluid is water, where $T_{\max}$ is the temperature at which water has maximum density (4.03°C) and q is 1.894816.

III. Numerical Solution Procedure

A. Discretization of Governing Equations

The two-dimensional governing equations are discretized by applying a finite volume method [15], in which conservation laws are applied over finite-sized control volumes around grid points, and the governing equations are then integrated over the control volume. Staggered grid arrangement is used in discretization of the computational domain in momentum equations. A power law

scheme is used to discretize convection/diffusion terms in momentum and energy equations. The main algebraic equation resulting from this control-volume approach is in the form of

$$a_P\phi_P = \sum a_{nb}\phi_{nb} + b \tag{22}$$

where ϕ_P represents the value of variable ϕ (U, V, or T) at the grid point P, ϕ_{nb} are the values of the variable at P's neighbor grid points, and a_P, a_{nb}, and b are corresponding coefficients and terms derived from original governing equations. The numerical simulation is accomplished by using SIMPLE algorithm [15]. The velocity-correction equations for corrected U and V in the algorithm are

$$U_e = U_e^* + d_e(P'_P - P'_E) \tag{23}$$

$$V_n = V_n^* + d_n(P'_P - P'_N) \tag{24}$$

where, according to the staggered grid arrangement, e and n, respectively, represent the control-volume faces between grid P and its east neighbor E and grid P and its north neighbor N. The source term S in governing equations is linearized into the form

$$S = S_C + S_P\phi_P \tag{25}$$

in a control volume, and by discretization, S_P and S_C are then, respectively, included in a_P and b in Eq. (22).

B. Ramped Switch-Off Method

To avoid discontinuity of the values of U and V at the phase-change fronts, Ma and Zhang [14] developed a RSOM in which the whole domain is divided into three regions: solid region, mushy region, and liquid region. In the solid region ($T \le -\Delta T$), the value of a_P is set as a very large positive number, 10^{30}, whereas d_e and d_n are set as very small positive numbers, 10^{-30}. In the mushy region where $-\Delta T \le T \le \Delta T$, the adjustments for a_P, d_e, and d_n satisfy the following linear relations:

$$a_P = a_{Pi} + \frac{T - \Delta T}{2\Delta T}(a_{Pi} - 10^{30}) \tag{27}$$

$$d_e = d_{ei}/a_P, \qquad d_n = d_{ni}/a_P \tag{28}$$

where a_{Pi}, d_{ei}, and d_{ni} are the values of these coefficients in the mushy region originally computed by SIMPLE algorithm. For the liquid area ($T \ge \Delta T$), a_P, d_e, and d_n are just directly computed by the SIMPLE algorithm.

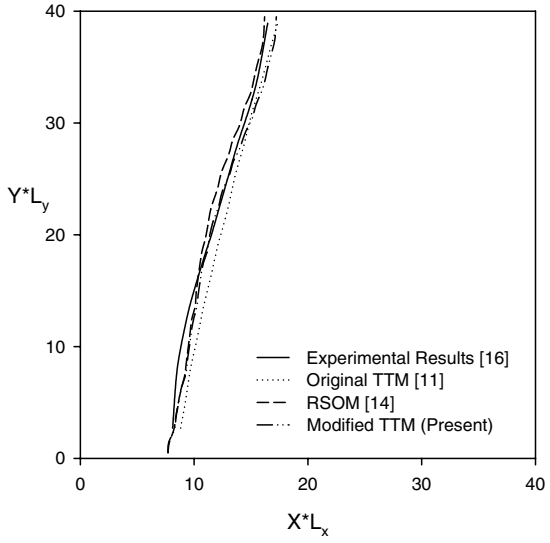

Fig. 2 Comparison of the locations of the melting fronts at $\tau = 39.9$.

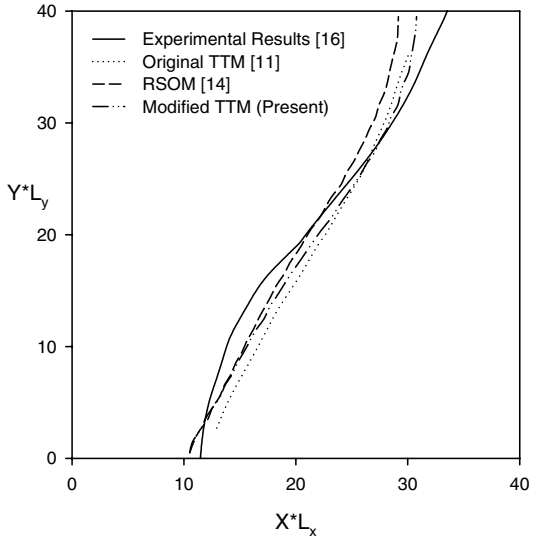

Fig. 3 Comparison of the locations of the melting fronts at $\tau = 78.68$.

IV. Results and Discussions

The TTM was validated by comparing its results to an experimental result and other numerical results. Figure 2 shows the positions of melting fronts obtained by the modified TTM compared with Okada's experimental results [16], Cao and Faghri's TTM simulation [11], and Ma and Zhang's numerical results [14] at a dimensionless time of $\tau = 39.9$. The PCM used in those researches were octadecane (which has a solid–liquid heat capacity ratio of 0.986), thermal conductivity ratio of 2.355, and Prandtl number of 56.2. All cases started with a temperature very close to the melting point, in other words, the subcooling parameter was equal to 0.01, the Stefan number was 0.045, and the Raleigh number was 10^6. The width of the mushy zone $2\Delta T$ was assumed to be 0.02. Following the suggestion by Ma and Zhang [14], the grid number of 40×40 and time step of 0.1 were used for this step. Although the heat capacity ratio of octadecane is very close to one, the modified TTM results show a slight improvement by moving closer toward experimental results in [16]. Even though modified TTM requires more iterations (216,729 iterations) than the original TTM (211,264 iterations), the difference in number of iterations between both methods is not very significant. Figure 3 shows those positions at $\tau = 78.6$. As time

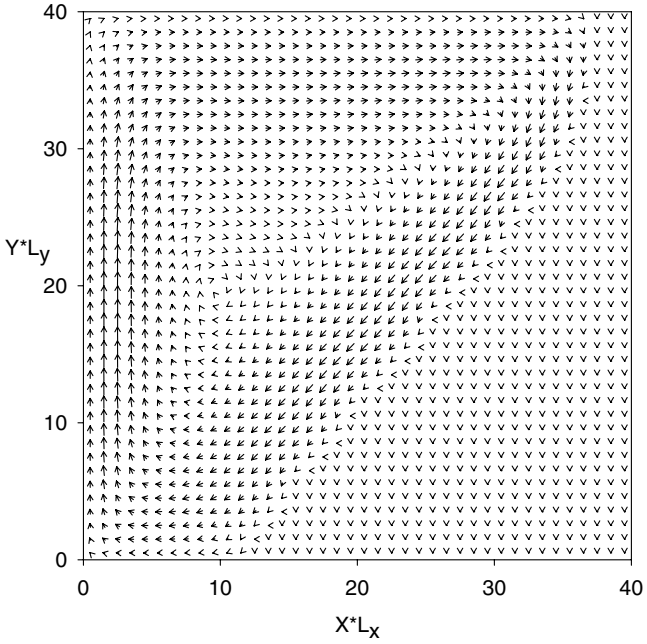

Fig. 4 Velocity vector when $\tau = 78.68$ for modified TTM.

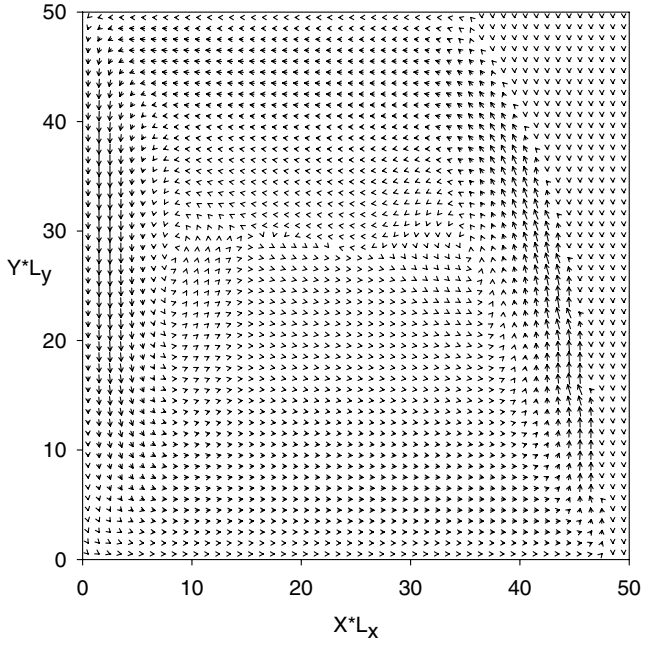

a) $T_h = T_{max} = 4.03°C$

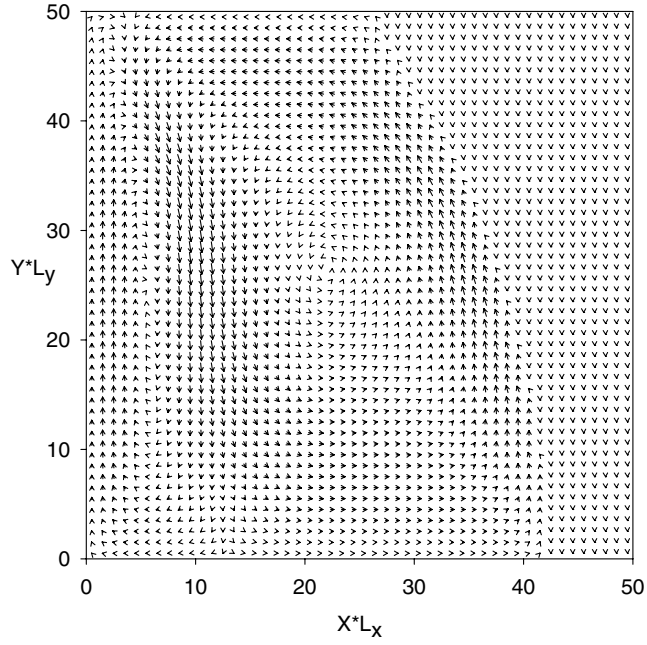

b) $T_h = 8°C > T_{max}$

Fig. 5 Velocity vector plot at $\tau = 57.7$ shows the unique ability of water flow in different temperatures on the right wall.

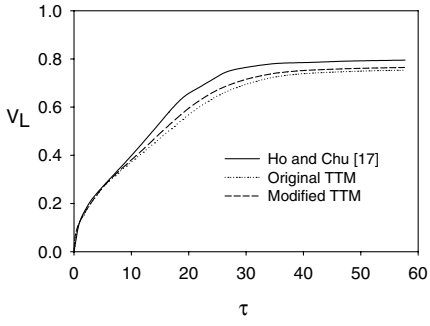

a) Melting rate

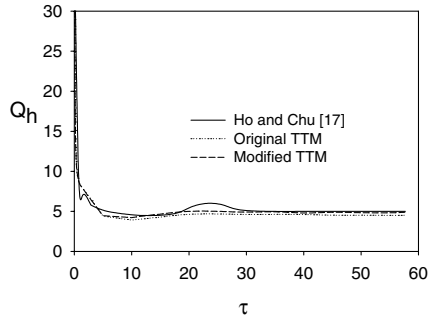

b) Heat transfer rate on the left wall

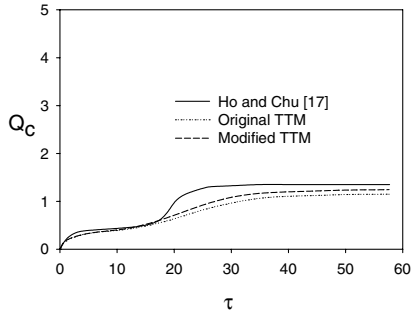

c) Heat transfer rate on the right wall

Fig. 6 Comparison of volume fraction and total heat on right and left walls for water ($C_{sl} = 0.477$, $K_{sl} = 3.793$).

progresses, the modified TTM gives results closer to the experimental result. The velocity vector contour for $\tau = 78.6$ is given in Fig. 4. It can be seen that the liquid flows upward near the heated wall and flows downward near the solid–liquid interface, which is consistent with the typical natural convection problem with higher temperature on the left wall. The modified TTM with RSOM can provide accurate prediction for phase-change problems with natural convection.

The modified TTM with RSOM is further tested with substances that have the heat capacity ratio far from one. The substance of choice is water, which has C_{sl} of 0.477, K_{sl} of 3.793, and Prandtl number of 11.54. The Sc is 0.25, the ΔT of 0.03, and the Ste is 0.101. After extensive grid-dependent study, a 50×50 grid and time step size of 10^{-4} were chosen as the optimum grid and time step for modified TTM to be applied with water. Figure 5 shows the velocity vectors at different heating temperatures. It can be seen that the modified TTM can capture the unique flow pattern of water: water has one circulation when temperature is less than 4.03°C (the temperature with highest density) and it has two circulations when temperature is higher than 4.03°C. Figure 6 shows the comparison of total volume fraction V_L, total heat on the left wall Q_h, and total heat on the right wall Q_c between modified and original TTM results to those of Ho and Chu [17]. In [17], Ho and Chu used a hybrid method in which temperatures were solved separately for solid and liquid regions, but on a fixed grid over the entire domain, whereas TTM methods use one equation for temperature over a fixed grid domain. In the comparison, the same grid and time step sizes are used in all three methods. Both modified and original TTM underpredict total heat transfer inside the domain when comparing with [17]. However, modified TTM still gives results closer to [17] than the original TTM. Figure 7 shows the comparison of the locations of the solid–liquid interface obtained by different models. It can be seen that the original TTM underpredicts the melting rate of substance, with the heat capacity ratio less then one.

Finally, melting of a substance with the heat capacity ratio higher than one (acetic acid, $C_{sl} = 1.203$) was studied. The acetic acid has K_{sl} of 1.2 and Prandtl number of 14.264. The Stefan number is chosen to be 0.045 and ΔT is 0.01. The optimum grid size for melting of acetic acid cases is 40×40 and the time step is 0.1. Because the original TTM uses the average of heat capacity in the mushy zone and it underpredicts the total heat transfer when the heat capacity ratio is less than one, and so the opposite effect is expected when the ratio is

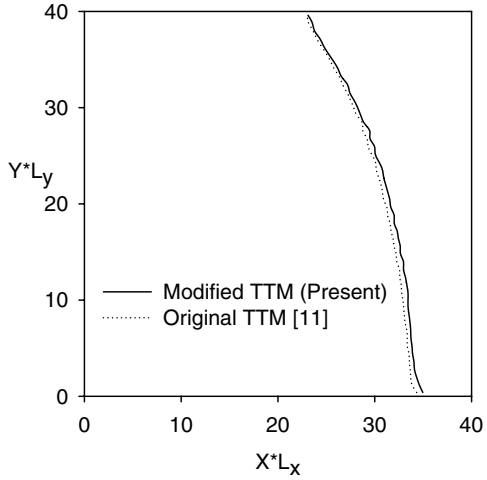

Fig. 7 Comparison of the locations of the melting fronts for water at time 57.7 ($C_{sl} = 0.477$, $K_{sl} = 3.793$) with $T_h = 8°C$.

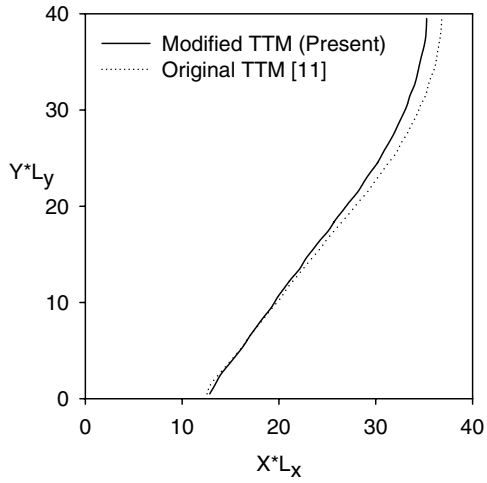

Fig. 8 Comparison of the locations of the melting fronts for acetic acid at time 100 ($C_{sl} = 1.203$, $K_{sl} = 1.2$).

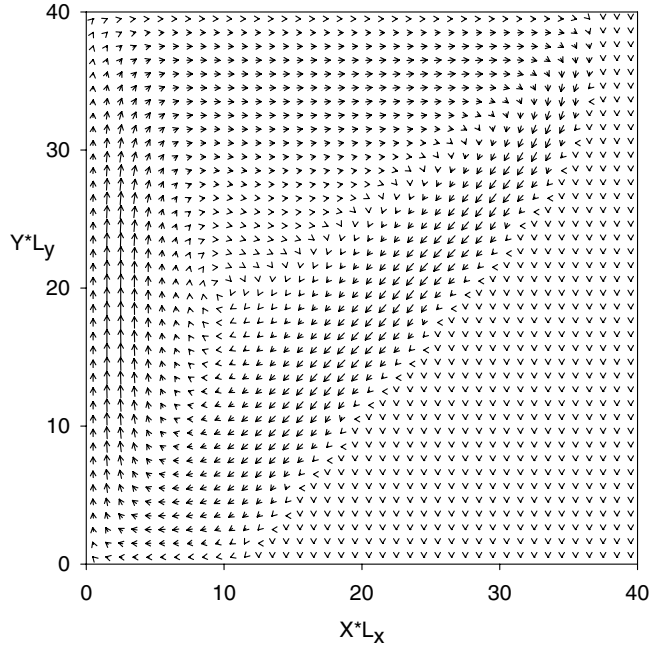

Fig. 9 Velocity vector for acetic acid at time 57.7 ($C_{sl} = 1.203$, $K_{sl} = 1.2$).

higher than one. Figure 8 shows that the original TTM overpredicts the movement of solid–liquid interface when the working fluid has the heat capacity ratio higher than one. Figure 9 shows the velocity vector for the acetic acid flow inside the rectangular cavity, which is also consistent with conventional natural convection with high temperature at the left wall.

V. Conclusions

A modified TTM was proposed and numerical simulation for three substances were carried out. Even for the PCM with the heat capacity ratio close to one, the present model yields results closer to the experimental results than the original TTM. The difference in predicted melting rate becomes larger when the heat capacity ratio is further away from one and the modified TTM will give better prediction than the original TTM. The original TTM underpredict the location of the interface when the heat capacity ratio is less than one and it will overpredict when the ratio is larger than one.

References

[1] Yao, L. C., and Prusa, J., "Melting and Freezing," *Advances in Heat Transfer*, Vol. 25, No. 1, 1989, pp. 1–96.

[2] Faghri, A., and Zhang, Y., *Transport Phenomena in Multiphase Systems*, Elsevier, New York, 2006.

[3] Zhang, Y., and Faghri, A., "Semi-Analytical Solution of Thermal Energy Storage System with Conjugate Laminar Forced Convection," *International Journal of Heat and Mass Transfer*, Vol. 39, No. 4, 1996, pp. 717–724.

[4] Zhang, Y., and Faghri, A., "Heat Transfer Enhancement in Latent Heat Thermal Energy Storage System by Using the Internally Finned Tube," *International Journal of Heat and Mass Transfer*, Vol. 39, No. 15, 1996, pp. 3165–3173.

[5] Zhang, Y., and Faghri, A., "Heat Transfer Enhancement in Latent Heat Thermal Energy Storage System by Using an External Radial Finned Tube," *Journal of Enhanced Heat Transfer*, Vol. 3, No. 2, 1996, pp. 119–127.

[6] Voller, V. R., "An Overview of Numerical Methods for Solving Phase Change Problems," in *Advances in Numerical Heat Transfer*, edited by W. J. Minkowycz, and E. M. Sparrow, Vol. 1, Taylor and Francis, Washington, D.C., 1997.

[7] Sasaguchi, K., Ishihara, A., and Zhang, H., "Numerical Study on Utilization of Melting of Phase Change Material for Cooling of a Heated Surface at a Constant Rate," *Numerical Heat Transfer*, Vol. 29, Part A, 1996, pp. 19–31.

[8] Binet, B., and Lacroix, M., "Melting from Heat Sources Flush Mounted on a Conducting Vertical Wall," *International Journal of Numerical Methods for Heat and Fluid Flow*, Vol. 10, No. 3, 2000, pp. 286–306.

[9] Morgan, K., "A Numerical Analysis of Freezing and Melting with Convection," *Computer Methods in Applied Mechanics and Engineering*, Vol. 28, No. 3, 1981, pp. 275–284.

[10] Hsiao, J. S., "An Efficient Algorithm for Finite Difference Analysis of Heat Transfer with Melting and Solidification," ASME Paper 84-WA/HT-42, 1984.

[11] Cao, Y., and Faghri, A., "A Numerical Analysis of Phase Change Problem Including Natural Convection," *Journal of Heat Transfer*, Vol. 112, No. 3, 1990, pp. 812–815.

[12] Voller, V. R., "An Enthalpy Method for Convection/Diffusion Phase Change," *International Journal for Numerical Methods in Engineering*, Vol. 24, No. 1, 1987, pp. 271–284.

[13] Yang, M., and Tao, W. Q., "Numerical Study of Natural Convection Heat Transfer in a Cylindrical Envelope with Internal Concentric Slotted Hollow Cylinder," *Numerical Heat Transfer*, Vol. 22, Part A, 1992, pp. 289–305.

[14] Ma, Z., and Zhang, Y., "Effects of Solid Velocity Correction Schemes on a Temperature Transforming Model for Convection Controlled Solid-Liquid Phase Change Problems," *International Journal of Numerical Methods for Heat and Fluid Flow* (to be published).

[15] Pantankar, S. V., *Numerical Heat Transfer and Fluid Flow*, McGraw–Hill, New York, 1980.

[16] Okada, M., "Analysis of Heat Transfer During Melting from a Vertical Wall," *International Journal of Heat and Mass Transfer*, Vol. 27, No. 11, 1984, pp. 2057–2066.

[17] Ho, C. J., and Chu, C. H., "The Melting Process of Ice from a Vertical Wall with Time-Periodic Temperature Perturbation Inside a Rectangular Enclosure," *International Journal of Heat and Mass Transfer*, Vol. 36, No. 16, 1993, pp. 3171–3186.